Cold Regions Science and Technology 213 (2023) 103902

Contents lists available at ScienceDirect

Cold Regions Science and Technology

journal homepage: www.elsevier.com/locate/coldregions

Hydraulic conductivity of fine-grained soils subjected to freeze-thaw cycles

Shuyin Feng [a], Erdin Ibraim [b], Paul J. Vardanega [b,*]

[a] Faculty of Computing, Engineering and the Built Environment, Birmingham City University, Birmingham B4 7XG, UK
[b] Department of Civil Engineering, University of Bristol, Bristol BS8 1TR, UK

ARTICLE INFO

Keywords:
Freeze-thaw
Clays
Atterberg limits
Hydraulic conductivity

ABSTRACT

This paper presents laboratory data from tests on four fine-grained soils: reconstituted Kaolinite, destructured Bothkennar clay, reconstituted Bothkennar clay, and reconstituted Gault clay. The soil samples were conditioned in an oedometer cell while being subjected to varying numbers of freezing and thawing cycles. The influence of freeze-thaw cycles on key soil parameters, including the hydraulic conductivity, Atterberg limits, compression and swelling index was studied. The experimental results were then compared with the analysis of a previously published database of hydraulic conductivity measurements on fine-grained soils called FG/KSAT-1358. The paper demonstrates that while multiple cycles of freezing and thawing affect some of the studied soil parameters, such as the Atterberg limits and the compression characteristics, the effects on the hydraulic conductivity transformation model parameters, linking the water content ratio to hydraulic conductivity are less apparent. The results are useful for geotechnical and pavement engineers when making assessments of freeze-thaw effects on subgrade materials in cold regions.

1. Introduction

1.1. Literature review

The hydraulic conductivity (k) is an important indicator of pavement material performance (cf., Dawson, 2009), and therefore a reliable assessment of k is often required during pavement design and assessment (cf. Mallick and El-Korchi (2008), Thom (2014)). However, unlike other geotechnical underground structures, the road pavement is usually directly exposed to ambient climate conditions such as temperature variation and precipitation which may lead to significant changes in subgrade soil properties (e.g., Simonsen and Isacsson (1999), Sarsembayeva and Collins (2017), Tripathy et al. (2020)). For road pavements constructed in cold regions where ice (or snow) is present for part of the year, the subgrade soil can be subjected to multiple freeze and thaw cycles during its service life. Henry (2007) explained that future research on the accumulated effect from multiple cycles of freezing and thawing are of interest as the frequency of soil cyclic freezing and thawing is increasing due to changes in climate. The k level influences the water accumulation during the freezing period and the moisture redistribution in the thawing period (e.g., Jones (1987), Wong and Haug (1991), Simonsen and Isacsson (1999), Mallick and El-Korchi (2008), Dawson (2009)), while freeze-thaw may lead to concomitant changes in k (e.g., Chamberlain and Gow (1979), Konrad (1989), Wong and Haug (1991), Benson and Othman (1993), Hewitt and Daniel (1997), Viklander (1997), Konrad (2010)) and other pertinent characteristics, such as the void ratio (e), Atterberg limits, apparent soil cohesion, and mean particle size (e.g., McDowall (1960), Yong et al. (1985), Eigenbrod et al. (1996), Viklander (1997), Hohmann-Porebska (2002)). For more detailed information, Table 1 gives a summary of many freeze-thaw studies on various soil types, and summarises the parameters investigated by the authors of the listed papers. The effects of freezing and thawing on the k of soils (in particular for fine-grained soil) have been the subject of many studies as listed in Table 1 which details the soil types, freezing and k measurements conditions, freeze-thaw cycle numbers and summary of the conclusions of the reviewed studies.

Examination of Table 1 reveals the following high level observations: (i) freezing and thawing conditioning may lead to significant changes in the k of soil to varying degrees and up to several orders of magnitude depending on both the soil type and the freezing and thawing conditions (e.g., Benson et al. (1995), Viklander (1998)); (ii) some studies showed that there is little change in k when the number of freeze-thaw cycles applied to the samples exceed three to twelve (e.g., Othman and Benson (1993), Jamshidi et al. (2015)); (iii) some of the listed studies revealed unfrozen and freeze-thaw conditioned soil samples may exhibit different log(k) - e correlations (e.g., Chamberlain et al. (1990), Konrad (2010)).

* Corresponding author.
E-mail address: p.j.vardanega@bristol.ac.uk (P.J. Vardanega).

https://doi.org/10.1016/j.coldregions.2023.103902
Received 21 September 2022; Received in revised form 15 May 2023; Accepted 20 May 2023
Available online 22 May 2023

Notation list

The following notation is used in this paper (units in brackets L = length, T = time and M = mass):

C_C	compression index
C_S	swelling index
c_v	coefficient of consolidation (L^2. T^{-1})
COV	coefficient of variation
D_{10}	particle size for which 10% of the soil is finer (L)
D_{30}	particle size for which 30% of the soil is finer (L)
D_{60}	particle size for which 60% of the soil is finer (L)
D_{90}	particle size for which 90% of the soil is finer (L)
e	void ratio
e_L	void ratio at w_L
G_S	specific gravity
I_P	plasticity index ($I_P = w_L$ - w_P)
k	hydraulic conductivity ($L.T^{-1}$)
k_{sat}	saturated hydraulic conductivity ($L.T^{-1}$)
LVDT	linear variable differential transformer
m_v	coefficient of volume compressibility (L. T^2. M^{-1})
n	number of data points
p	p–value
R^2	coefficient of determination
SE	standard error
w	water content
w/w_L	water content ratio
w_L	liquid limit
w_P	plastic limit
γ_w	unit weight of the permeant (M. L^{-2} T^{-2})
μ	mean
σ	standard deviation

1.2. Database study of fine-grained soil hydraulic conductivity

Feng and Vardanega (2019a, 2019b) presented a database (FG/KSAT-1358) of k measurements along with other soil index parameters from 1358 tests on over 30 fine-grained soils. The database can be freely downloaded from the TC304 databases (http://140.112.12.21/issmge/tc304.htm). Correlations linking the liquid limit (w_L), e, with k were established using the database and further simplification led to a transformation model using the w/w_L (w/w_L can also be correlated with e.g. undrained shear strength: Kuriakose et al. (2017)) as the predictor for k (see Feng and Vardanega (2019b) and the discussion in Feng and Vardanega (2019a)). Nagaraj et al. (1993, 1994), used e normalized with the e at w_L (e_L) (e/e_L) for developing correlations linking k to e/e_L. Sivapullaiah et al. (2000) and Mbonimpa et al. (2002) also used a similar approach using e/e_L for the prediction of k. The calibrated transformation model from Feng and Vardanega (2019b) is given as Eq. (1):

$$k_{sat}(m/s) = 1.91 \times 10^{-9}(w/w_L)^{4.083} \quad (1)$$

Feng et al. (2022) further investigated the influence of statistical outliers in the database FG/KSAT-1358 on the regression model and demonstrated that the regression coefficient and exponent of the adjusted model (1.86×10^{-9}, 4.226) are similar to those in Eq. (1) (1.91×10^{-9}, 4.083).

The soil k can be determined through both direct measurements (e.g., constant head test, falling head test) and indirect assessment by interpreting the coefficient of consolidation (c_v) data from the step-loaded oedometer test based on Terzaghi's theory of consolidation (e.g., Tavenas et al. (1983), Craig (2004), Chapuis (2012)). Eq. (1) is based on data from four approaches for measuring k: falling head test ($n = 580$), constant head test ($n = 169$), consolidation test ($n = 512$), and flow-pump test ($n = 91$). Considering that the k values in this study are all inferred from consolidation test data, the test results are compared to the consolidation test data in FG/KSAT-1358, the transformation model based on the consolidation test data subset ($n = 512$) from FG/KSAT-1358 was found in Feng and Vardanega (2019b) to be:

$$k_{sat}(m/s) = 1.00 \times 10^{-9}(w/w_L)^{3.75} \quad (2)$$

1.3. Research aims

The research has three key aims:

(1) Examine key soil properties (including classification parameters and soil compression indices) to see if they are significantly affected by freezing and thawing cycles and compare this with the effect of sample state (in this case reconstituted or destructured) on the measured compression indices.

(2) Examine the transformation model parameters that link w/w_L to k_{sat} (see Eqs. 1 and 2) and investigate if they are affected by multiple cycles of freezing and thawing and if these parameters affected by sample state.

(3) Determine if the transformation models (see Eqs. 1 and 2) which can be used predict k_{sat} from w/w_L remain sufficiently accurate when data from soils subjected to multiple cycles of freezing and thawing are included in the calibration datasets.

2. Experimental methodology

To achieve the research aims stated in Section 1.3, an experimental campaign consisting of a series of soil index tests and k measurements on fine-grained soil samples was conducted. The samples were fabricated from three different origin soils and conditioned by various numbers of freezing and thawing cycles. For more details on the experimental methodology and testing results, see the thesis of Feng (2022).

2.1. Tested materials

Speswhite Kaolin, Bothkennar clay, and Gault clay were used in the laboratory testing programme. The Speswhite Kaolin used in this study is an industrially available laboratory soil. Kaolin generally has little organic content as it is formed from crystalline rocks (Prasad et al., 1991). More details of the soil index properties measured on the tested Kaolin are given in Table 2. The tested (unconditioned) Kaolin in this study is classified as a high plasticity clay based on BS EN ISO 14688-2:2018 (British Standards Institution (BSI), 1990) (see Table 2) (later it will be shown that the Kaolin once subjected to various cycles of freezing and thawing may plot below the A-line on the Casagrande plot and hence be classified as a silt).

The Bothkennar clay used in this study was available from sealed Sherbrooke block sample cored at a depth of 4.35 m to 4.65 m from the Bothkennar Test Site (see the thesis of Sukolrat (2007)). The sampled soil block had been wax sealed over plastic film wrapping and stored in a cool, humid storeroom at the University of Bristol Geomechanics Laboratory. The measured organic content and the Atterberg limits are within the range given in Hight et al. (1992) and Nash et al. (1992) (cf. Table 2). The examined Bothkennar clay tested in this study is classified as high plasticity clay based on BS EN ISO 14688-2:2018 (BSI, 2018a) (see Table 2).

Gault clay was formed "in a deepening muddy sea" and is usually in blue grey colour (Pennington, 1999, p. 48). The Gault clay used in this study was from a sample block stored in the University of Bristol Geomechanics laboratory in the same storeroom as the Bothkennar block sample. The sample was poorly sealed, exposed to air, without any legible information on the sample location and year. The soil index

Table 1
Summary of past studies reported in the literature.

Source	Soil types	Soil parameters	*k* test type	Freezing type	T_F (°C)*	Max. cycles	Summary
Chamberlain and Gow (1979)	Ellsworth clay, Morin clay, CRREL clay, and Hanover silt.	Vertical *k*	Constant head	Unidirectional bottom to top, open system		5	• Vertical *k* increases after freezing and thawing • The increase in *k* is higher for soil with higher I_P and smaller at the highest applied stress level [data from this source was previously included in FG/KSAT/1378, see Feng and Vardanega, 2019b]
Chamberlain et al. (1990)	Silt loam clay (high plasticity clay), clay loam (silt)	*k*	Falling head EM 1110–2-1906	Unidirectional bottom to top, with water access from the top, open system		15	• *k* is not always related to the number of freeze-thaw cycles • Higher initial *w* will lead to larger increases in *k* after freezing and thawing • Most changes in *k* occurred in the first nine cycles • Highly compacted sample will experience smaller change in both *e* and *k* after freezing and thawing
Wong and Haug (1991)	Sand, till and sand-bentonite mixture	*k*	Flexible wall/fixed wall constant head	Closed system	-20	5	• The *k* of the clay liner examined increased with increasing freezing and thawing cycles, however the rate of increase diminished with each subsequent cycle • Most changes in *k* of till liner occurs during the first freezing and thawing cycle • The closed system freeze/thaw condition has little influence on the compacted Ottawa sand and sodium bentonite • The inclusion of 25% sodium bentonite did not increase the frost susceptibility Ottawa sand
Kim and Daniel (1992)	Glacially derived clay	*k*, *e*	Flexible wall permeameter test ASTM 5084	Three dimensional in an environmental chamber, closed system	−17.8	5	• Molding *w* greatly influenced the effect of freeze-thaw cycles on *k* • Samples compacted under wet of optimum condition experienced greater increases in *k* • Freeze-thaw cycles created more fluid-conducting pores in soils
LaPlante and Zimmie (1992)	Niagara clay, Brown clay	*k*	Flexible wall	Both unidirectional and three dimensional		19	• The maximum change in *k* occurred within the first 10 cycles • Changes in *k* are related to the effective stress, with changes up to two orders of magnitude under low effective stress condition • Changes in *k* due to freeze/thaw condition can be eliminated by landfill operation within the first year
Benson and Othman (1993)	Glacial clay	*k*	Flexible wall permeameter ASTM D5084 method D constant rate of flow test	In field, top to bottom, open system	−20	4	• The *k* of the soil above the freezing boundary is about one to two orders of magnitude greater than that before freezing occurred • Soil *k* about 150 mm below the freezing boundary was found to be about one order of magnitude higher than that before freezing occurred
Othman and Benson (1993)	Sand-Bentonite mixture, geosynthetic clay liner	*k*	Flexible wall permeameter constant head	Unidirectional closed system; Three dimensional closed system	−5	6	• Freezing under uni-direction or three-dimensional conditions has no significant influence on the ice structure obtained • Larger temperature gradient will induce bigger increases in *k* • Higher overburden stress might offset some of the effects brought by freezing and thawing cycles • The majority changes in soil structure and *k* occurred in the first three cycles

(*continued on next page*)

Table 1 (*continued*)

Source	Soil types	Soil parameters	*k* test type	Freezing type	T_F (°C)*	Max. cycles	Summary
Bowders and McClelland (1994)	Kaolinite, pulverized shale, residual clay soil	*k*	Flexible wall permeameter ASTM D5084 constant head	Three dimensional closed system	−18	24, 6, 1	• The increase in *k* of kaolinite and residual clay soil ranged from one to two order of magnitude after the freeze/thaw process • The magnitude of change in *k* after freeze-thaw process increased with increasing soil plasticity • The increase in *k* from freeze-thaw process is partially reversible by increasing the effective stress
Benson et al. (1995)	Glacial till	*k*	Sealed double-ring infiltrometer ASTM D5093 flexible wall permeameter ASTM D5084 method C falling head	Freeze in field; three dimensional closed system	−2.5	10	• The *k* of soil within the zone of freezing increased by 50 to 300 times its initial value • The changes in *k* of soil from freezing and thawing cycles measured from laboratory test are comparable to those occurred in the field
Hewitt and Daniel (1997)	Geosynthetic clay liner	*k*,	Flexible wall permeameter	Three dimensional closed system	−20	3	• Most geosynthetic clay can maintain low *k* after three freezing and thaw cycles
Viklander (1998)	Fine-grained nonplastic till	*k*, *e*	Rigid wall Permeameter Constant head	Unidirectional, bottom to top, closed system	−3	18	• The *k* of the initially dense samples increased by a factor of <2, while for initially loose samples, the *k* decreased by a factor of 1.4 to 3 • The residual *e* after 1 to 3 cycles for both initially dense and loose soils are about 0.31 to 0.4
Konrad and Samson (2000)	Kaolinite-silt mixture	*k*, *e*	Constant head	Bidirectional, closed system	−7.3 to −3.7	1	• Sample after 1 freezing thawing cycle exhibited an increase in *k* and a decrease in *e* • The change in *e* is relate to the temperature below which no further change appears in unfrozen *w* • The compressibility characteristics of thawed mixture is similar to the overconsolidated mixture • The ratio of change in *e* to change in log *k* for unfrozen sample is larger for unfrozen soil than thawed soil
Viklander and Eigenbrod (2000)	Silty sandy soil	*k*, stone heave	Falling head	Unidirectional, top to bottom, open system	−5 & -10	9	• Changes in *k* are more apparent for dense soils than for loose soils • For dense soil, *k* increases during the first three to four cycles but subsequently decreases • Both stone and soil heave is considerably higher in the open system freezing with free access to water than in the closed system • The amount of heave was highest in soil compacted at optimum *w*.
Konrad (2010)	Low plasticity glacial till	*k*	Constant head	Bidirectional, closed system	−5	4	• The change of *k* after repeated freezing and thawing is larger in unsaturated sample than in saturated sample • The freezing and thawing induced *k* change is related to the initial *e* level prior to freezing • The ratio of change in *e* to change in log *k* for unfrozen sample is larger for unfrozen soil than for thawed soil
Jamshidi and Lake (2015)	Cement stabilized soil	*k*, unconfined compressive strength (UCS)	Flexible wall permeameter ASTM-D5084 method A Constant head	Three dimensional in a freezer	−10 ± 1	12	• Both minor reduction and increase up to 5250 times in *k* were observed after exposure to freezing and thawing. • Mature samples (longer curing time) exhibited higher increase in *k* than immature samples • Decreases up to 58% and increases up to 14% were observed in UCS value

(*continued on next page*)

Table 1 (*continued*)

Source	Soil types	Soil parameters	*k* test type	Freezing type	T_F (°C)*	Max. cycles	Summary
							• Some degree of healing in *k* changes due to freezing and thawing was identified, however, full recovery of *k* was not observed
Jamshidi et al. (2015)	Cement stabilized silty sand	*k*, unconfined compressive strength (UCS)	Flexible wall permeameter ASTM-D5084 method A Constant head	Three dimensional open system	−2, −10, −20	4, 12	• Changes in *k* of cement stabilized silty sand after multiple freezing and thawing cycles can be up to three orders of magnitude • The number of freezing and thawing cycle, freezing temperature, and curing time before conditioning all influence the *k* and strength of the cement stabilized sample • Higher changes in *k* and compressive strength emerges at the end of the 12th cycle rather than the 4th cycle • Self-healing appears in samples exposed to high freezing temperature (−2 °C)
Sterpi (2015)	Clayey silt	*k*	Oedometer test Flexible wall permeameter test ASTM D5084, D2435	Three dimensional in a freezing room, closed system	−18	4	• Damage to soil structure caused by freezing is progressive and permanent, the increase in *k* caused by freezing is up to one order of magnitude • For sample compacted with higher energy, the effects of freezing could be eliminated by medium to high stress • Freezing action may damage clay particles and lead to changes in physical and mechanical properties
Tang and Yan (2015)	Remolded Shanghai forth later soil	*k*, microstructure	QT1–3 seepage pressure instrument	Unidirectional, closed system	−17.7	1	• Higher *w* leads to more obvious change in soil structure • Due to the increase in number of large pore and micro-cracks, the *k* increased by an order of magnitude after one freezing and thawing cycles • The soil particles after freezing and thawing cycle are flattened and directional arranged from a flocculent structure
Makusa et al. (2016)	stabilized dredged sediments	*k*, unconfined compressive strength (UCS)	Rigid wall constant head test ASTM D5856	Three dimensional with material of different thermal conductivity around the preferential side, tested under both semi closed and open system conditions	−25	5	• Treated sediments with initially low UCS exhibited temporary reduction of UCS with an increase of *k* • Initially treated sediments with high UCS exhibited a permanent reduction of UCS without an increase in *k* • Open system freeze-thaw shortened the effect of thaw weakening, prolonged thaw weakening period might induce a reduction in strength

* T_F (°C) stands for the freezing temperature.

Table 2
Summary of the basic properties of the unconditioned soils.

Soil	Basic properties of the tested soils								
	G_S	w_L (%)	w_P (%)	Organic content (%)	D_{10} (μm)	D_{30} (μm)	D_{60} (μm)	D_{90} (μm)	Classification (BSI, 2018a)
Kaolin	2.63	68%	30%	0.8%	1.85	3.16	5.59	14.39	ClH (High plasticity clay)
Bothkennar	2.66	68%	29%	3.9%	3.94	8.72	19.38	53.65	ClH (High plasticity clay)
Gault	2.68	74%	25%	3.5%	2.17	3.73	7.54	28.89	ClV (Very high plasticity clay)

values measured for the Gault clay sample are summarised in Table 2. The tested Gault clay was classified as very high plasticity clay based on BS EN ISO 14688-2:2018 classification (BSI, 2018a) (see Table 2). The measured index values generally are within the range reported by Forster et al. (1995). The w_L of the examined Gault clay sample (74%) is generally within the range of results from the previous studies (i.e.

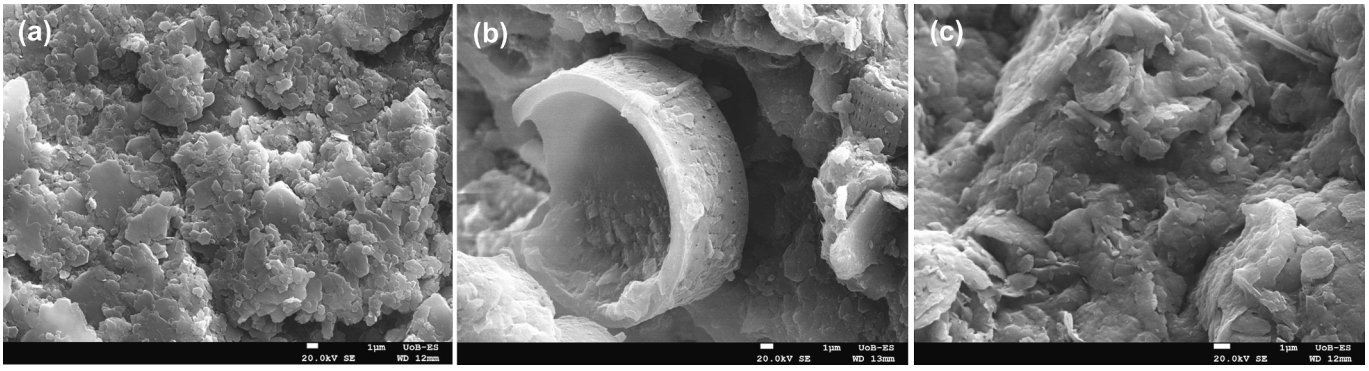

Fig. 1. Microstructure (SEM pictures) of the examined soil: (a) Kaolin, (b) Bothkennar clay, (c) Gault clay.

Table 3
Measured void ratio of the pre-conditioned oedometer samples (* *w* measured by batch before saturation).

Bothkennar- destructured		Kaolin- reconstituted			Bothkennar- reconstituted			Gault- reconstituted		
e	*w*	Batch*	*e*	*w*	Batch	*e*	*w*	Batch	*e*	*w*
1.79	68%	A	1.28	47%	A	1.12	41%	A	1.21	45%
1.84	68%	A	1.28	47%	A	1.08	41%	A	1.22	45%
1.79	67%	A	1.30	47%	A	1.11	41%	A	1.20	45%
1.77	67%	A	1.31	47%	B	1.03	37%	A	1.23	45%
1.77	68%	A	1.31	47%	B	1.03	37%	A	1.23	45%
1.68	65%	A	1.28	47%	B	1.04	37%	A	1.22	45%
1.75	68%	A	1.37	47%	B	1.00	37%	B	1.16	42%
1.68	68%				B	1.00	37%	B	1.14	42%
1.75	64%				B	1.03	37%	C	1.25	46%
1.83	68%				C	1.08	41%	C	1.21	46%
1.75	64%				C	1.03	41%			
1.75	64%									
$\mu = 1.76$, $COV = 2.6\%$			$\mu = 1.30$, $COV = 2.3\%$			$\mu = 1.05$, $COV = 3.7\%$			$\mu = 1.21$, $COV = 2.6\%$	

53.9% to 89.2%, Forster et al. (1995); 75% to 80%, Pennington (1999)), despite the excessively long drying/ storage period.

Fig. 1 shows the microstructure of the soils used in this study determined using scanning electron microscopy (JXA-8530F Field Emission Electron Probe Microanalyzer). Fig. 1 shows that the Kaolin has a simple, organised layer structure, mostly formed by clay platelets in a hexagon shape (Fig. 1a). The Bothkennar clay used in this test shows a more open structure with embedded shell fragments, microfossils, and silt-sized grains (see Fig. 1b, as was also observed by Paul et al. (1992)). The Gault clay in this study has an interlocking microstructure with elongated mineral particles and potential microfossils (see Fig. 1c, as was also observed by Pennington (1999)).

2.2. Sample preparation, test set up and procedure

2.2.1. Destructured sample preparation

The state of the Bothkennar sample was judged to be 'destructured' following the states of structure of clayey soil defined by Leroueil et al. (1985) in the discussion of the paper by Carrier and Beckman (1984). The destructured samples were made only for the Bothkennar soil with the material available (as the Gault sample available was found to be poorly sealed and exposed to air for decades), with around 300 mm in height and 250 mm in diameter. The sample was removed from the cool humid storeroom in the laboratory and unwrapped before being cut into soil wedges, and further sliced down horizontally to a suitable size with a sharp knife for conventional oedometer sample preparation. Soil wedge slices without any obvious fissures or cracks were selected for further oedometer sample preparation. All the oedometer samples were cut vertically parallel to the field sampling direction using standard cutting rings of diameter around 75 mm (actual size ranging from 74.86 mm to 76.12 mm), and height of around 20 mm (actual size ranged from about 18.7 mm to 19.78 mm). Slightly damped enlarged porous stones with 2 kg extra weight were placed over the top of the cutting ring to minimize the potential swelling of the prepared sample before the conditioning process.

All the destructured samples of Bothkennar (12 in total) were prepared in a single batch (i.e., from a single prepared soil column). The *e* measured from the pre-conditioned destructured sample ranges from 1.68 to 1.84, with a mean value of 1.76 and a coefficient of variation (COV = population standard deviation (σ)/population mean (μ)) of 2.6%. The *e* and water content of the prepared samples are summarised in Table 3. The offcuts and remaining soil wedges were reserved for Atterberg limit testing and the preparation of the reconstituted soil samples.

2.2.2. Reconstituted sample preparation

Reconstituted soil samples were prepared for the tested soils (i.e. Kaolin, Bothkennar, Gault). All the reconstituted samples were prepared following the method described in the thesis of Feng (2022) under four vertical pressures, 30 kPa, 60 kPa, 120 kPa, and 180 kPa, with the first three vertical pressure each maintained for 48 h, and the final vertical pressure (180 kPa) for 120 h (five days) to ensure the completion of the consolidation process. During the period of consolidation, the floating ring was displaced continuously to break the accumulated shaft friction. The height of the consolidated sample was monitored every 24 h. By the completion of the consolidation period, the vertical pressure was removed to allow the sample to swell for another 48 h.

The extruded soil column from the consolidometer tube (150 mm to 175 mm in length) was horizontally positioned in a sample catcher and cut horizontally carefully using a wire saw into 6 or 7 soil cylinders, and further into oedometer samples using slightly greased cutting rings of about 20 mm in height and 75 mm in diameter. To reduce the potential swelling after sample cutting, a slightly damped enlarged porous stone with 2 kg extra weight was placed on top of the cutting ring after the

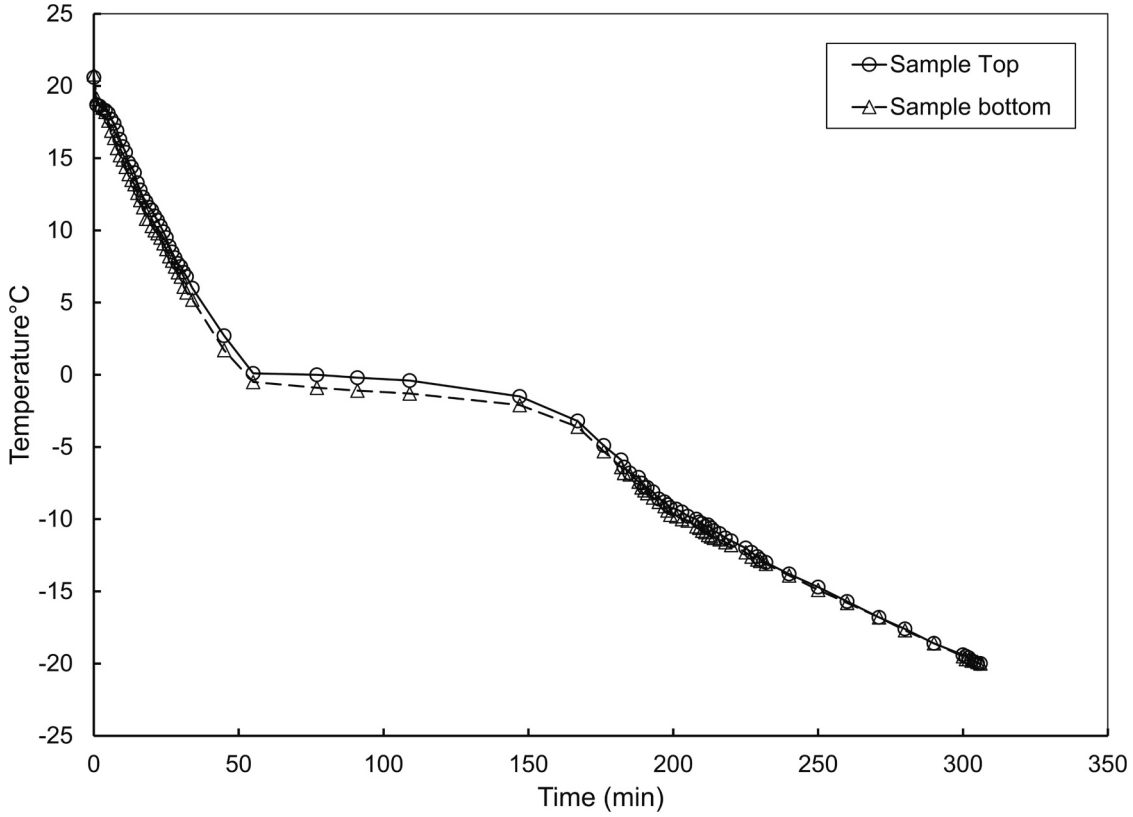

Fig. 2. Temperature variation of the sample during the freezing period.

Table 4
Freezing and thawing conditioning programme.

Freezing- thawing cycles	Number of Samples Conditioned			
	Destructured Sample	Reconstituted Sample		
	Bothkennar	Kaolin	Bothkennar	Gault
0	2	1	3	2
1	1	1	1	1
2	1	1	1	1
3	2	1	1	1
5	1	1	1	1
7	2	1	1	1
10	1	0	1	1
15	1	0	1	1
25	1	1	1	1
Total	12	7	11	10

final trimming and smoothing of the cut sample.

To distinguish the soil samples cut from different reconstituted soil column, all reconstituted samples were labeled with a batch number. The e measured from the pre-conditioned oedometer samples from different reconstituted batches in this study are presented in Table 3. It was noticed that some variation in e exists among the oedometer samples cut from different reconstituted soil columns and from different sections of the same soil column, *COV* of the post-cutting e is 2.6% for the reconstituted Gault sample, 3.7% for the reconstituted Bothkennar sample, and 2.3% for Kaolin (see Table 3).

2.2.3. Sample conditioning

The conditioning and testing procedures adopted for the reconstituted and the destructured samples were carefully followed throughout the experimental campaign. After sample preparation, the soil samples were kept in the cutting ring during the conditioning and testing processes to minimize sample disturbance.

The freezing condition of the soil can be classified as closed or open system depending on the accessibility of water during the freezing process (cf. Jones (1987)). Wong and Haug (1991) suggested that neither system can give an entirely appropriate simulation of field conditions, the choice of experiment condition should be made based on both the rate of frost penetration and rate of moisture transport, for soil with a k lower than 1×10^{-9} m/s, the closed system freezing may better represent field conditions (Wong and Haug, 1991). Othman and Benson (1993) indicated that no significant difference can be observed between the uni-directional or three-dimensional freezing condition in the conditioned soil samples. Benson et al. (1995) suggested that changes in k of soil subjected to three-dimensional freezing and thawing is comparable to the result measured in the field. Sarsembayeva and Collins (2017) suggested that the groundwater under the highway may include deicing agents (e.g., sodium chloride) during the subfreezing seasons, and the inclusion of deicing agents may lead to changes in soil property. As this research focused only on the influence of freezing and thawing conditioning, only clean de-ionized water was used for the conditioning and the subsequent k testing. Open system freezing with access of water was chosen as it was considered to be a better representation of the field condition, because the access of moisture for soil under freezing and thawing conditions is more likely than a completely isolated system. A mixture of both conditions probably exist during different phases and time intervals, however to simulate this in laboratory would be difficult to consistently achieve.

The test sample was conditioned inside a conventional oedometer cell with an internal depth of 45 mm, and an internal diameter of 115 mm (the exact size of each apparatus may vary slightly, as multiple oedometer cells were used in this experimental campaign), free access of water is provided from the bottom side through the porous stone. The cutting ring was fixed in place by the collar bolting system to prevent it from being lifted by sidewall friction. The total weight of the copper top cap and porous stone over each sample was measured to be around

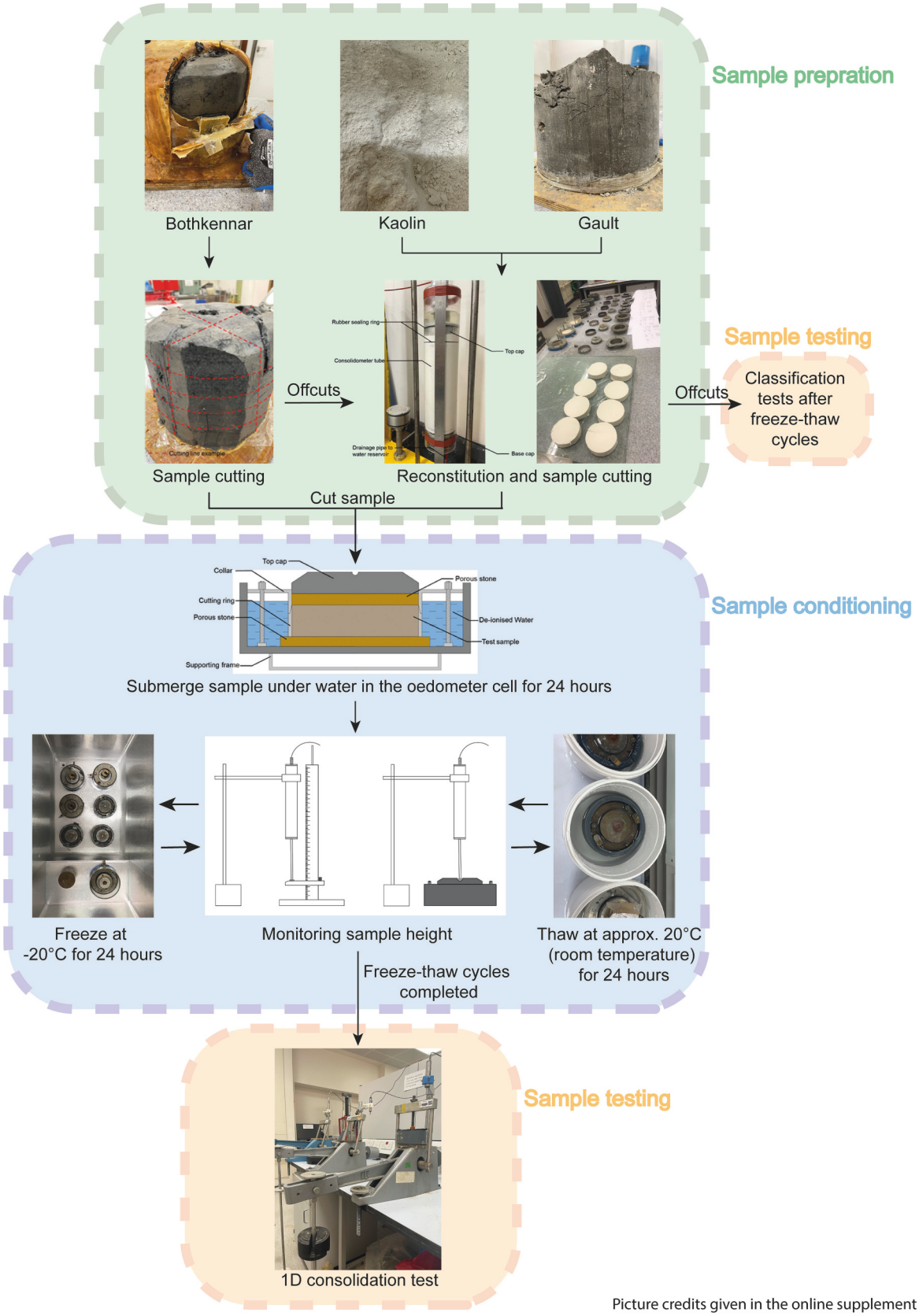

Fig. 3. Flowchart of the experiment process (see Figs. S1 to S11 of the supplemental data for original copies of the component images).

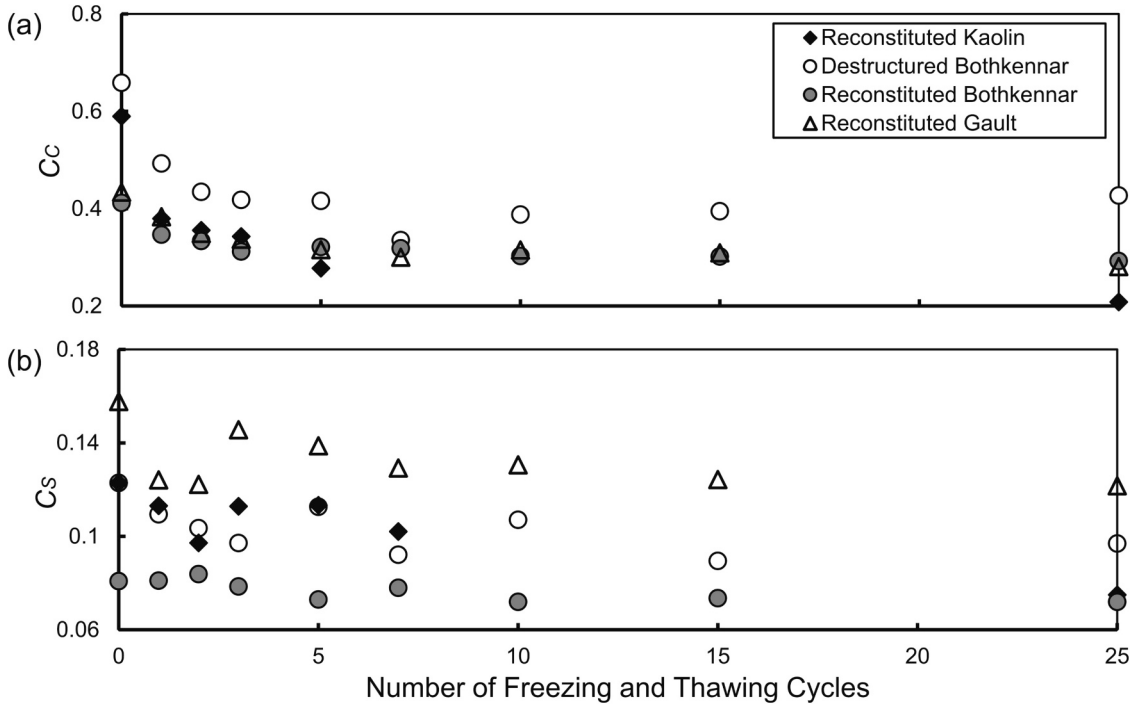

Fig. 4. Variation of compression/ swelling index over freezing and thawing cycles: (a) C_C variation, (b) C_S variation.

670 g. The sample was first submerged in de-ionized water in the oedometer cell to saturate for 24 h before placement in a freezer together with the oedometer cell. The temperature was set at −20 °C, the actual working temperature monitored inside the freezer cabinet fluctuated between −22.6 to −16.2 °C. Data of the temperature variation on both the top and bottom sides of the sample during the freezing period are shown in Fig. 2. After a continuous freezing period of 24 h, the oedometer cell was allowed to thaw with free access of water in a bucket at room temperature (approx. 20 °C) for 24 h. The bucket was half filled with water with its lid closed to maintain a high humidity environment. The sample height variations after each freezing or thawing phase were monitored throughout the experimental campaign, the height variation after each freezing phase and thawing phase for each sample type can be found in the supplementary data (see Figs. S12–S15).

For each soil type (destructured Bothkennar, reconstituted Kaolin, reconstituted Bothkennar, reconstituted Gault), soil samples were prepared and conditioned for up to 25 cycles of freezing and thawing, 40 samples were made and conditioned in total. Table 4 summarises the number of samples conditioned at different freezing and thawing cycles for each type of soil sample. Key soil parameters including the k_{sat}, Atterberg limits, compression and swelling indices of the conditioned samples were also measured. Fig. 3 summarises the sample preparation, conditioning, and testing processes.

2.3. Laboratory testing

2.3.1. One dimensional consolidation test

After completion of the designated cycles of freezing and thawing conditioning, the entire oedometer cell was installed into the one-dimensional loading frame, where the step loaded consolidation test was carried out to obtain the consolidation properties of the soil samples after different cycles of freezing and thawing conditioning. The test generally followed the procedures described in BS 1377–5:1990 (BSI, 1990) and generally complied to the subsequent BS EN ISO 17892-5:2017 (BSI, 2017). The soil sample after the last thawing phase of its designed cycles of freezing and thawing was consolidated under vertical incremental stresses of approximately 55 kPa, 110 kPa, 220 kPa, 440 kPa,1100 kPa, the exact value depending on the size of the cut sample which ranges from 74.86 mm to 76.12 mm (e.g., for 55 kPa, the actual stress applied can be around 54–56 kPa, for 1100 kPa, the range can be up to around 1078–1114 kPa). Each applied stress level was held for 24 h before moving to the next loading stage. On completion of the final loading stage, the sample was incrementally unloaded with each unloading stage sustained for 24 h. The height change of the tested sample was monitored throughout both the loading and unloading stages by using an LVDT sensor. The water temperature as monitored in the oedometer cell during the test was 21.5 ± 0.6 °C.

2.3.2. Hydraulic conductivity calculation

The k of the soil in consolidation was calculated using:

$$k = c_v m_v \gamma_w \tag{3}$$

where m_v ($L.T^2.M^{-1}$) is the coefficient of volume compressibility, γ_w ($M.L^{-2}.T^{-2}$) is the unit weight of the permeant (water), and c_v is the coefficient of consolidation, which can be determined from either the 'square root of time fitting method' (Taylor, 1948) or the 'logarithm of time fitting method' (attributed to 'Casagrande' by Craig (2004, p. 252), see also Olek (2019)). The k of the tested samples with a range of e values were assessed from oedometer test data using the Taylor's 'square root of time fitting method'. Detailed discussion on the choice of k measurement approaches is included in Feng (2022).

2.3.3. Classification tests

Soil classification tests were carried out to determine w_L, plastic limit (w_p), particle size distribution, and particle density of the tested soils. The tests conducted largely followed the BS 1377–2:1990 (British Standards Institution (BSI), 1990) and generally complied to the subsequent BS EN ISO 17892-12:2018 testing standard (BSI, 2018b), in which the cone penetrometer method with 30°/80 g cone was chosen for the w_L testing, the small pycnometer method was used for the particle density examination. The particle size distributions were examined using the laser diffraction particle size analyzer (Mastersizer 3000) available at the University of Bristol, the particle size distribution of the tested soils is available in the supplemental data (Fig. S16). The organic

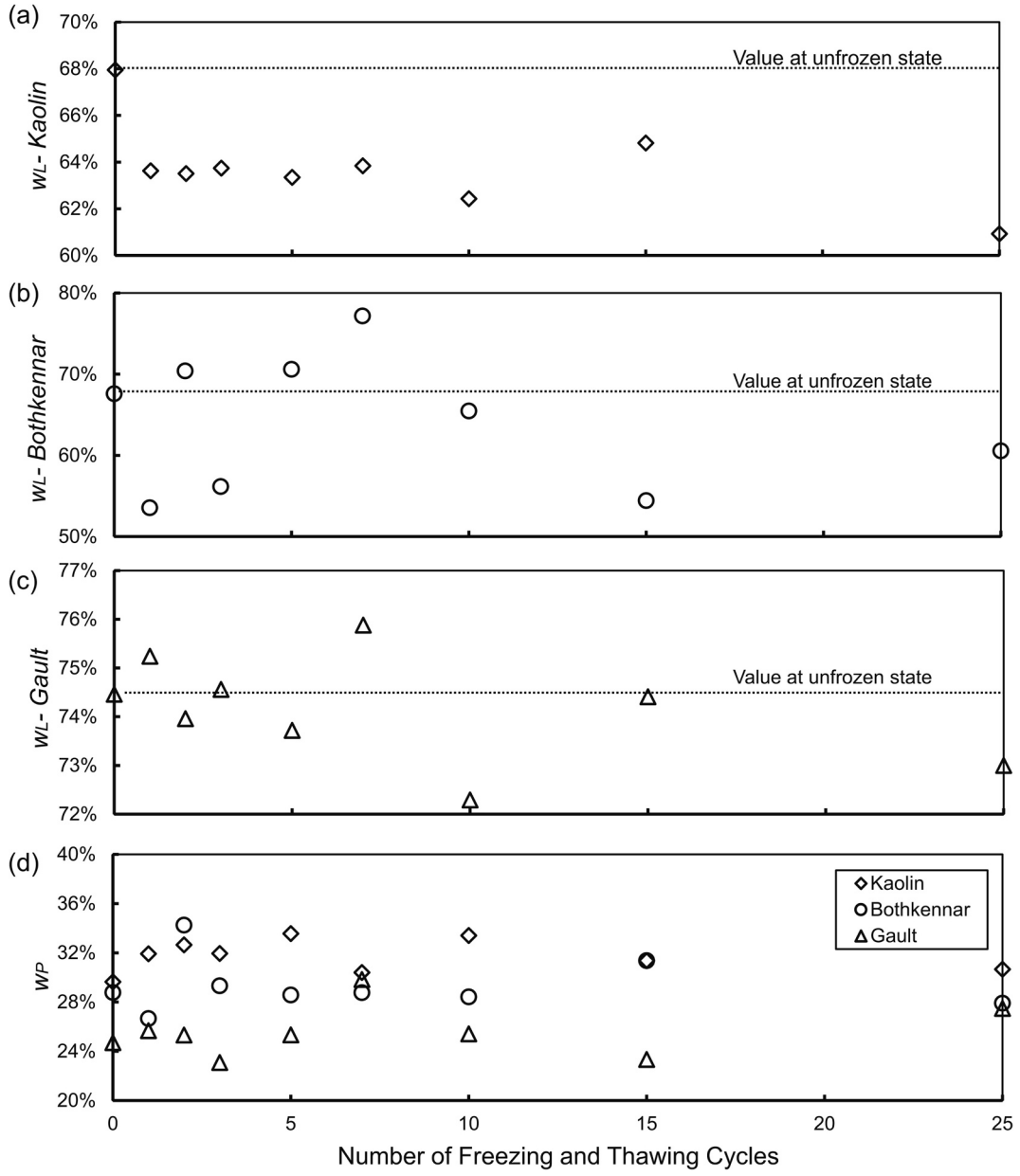

Fig. 5. Variation of w_L and w_P over freezing and thawing cycles: (a) to (c) w_L variation, (d) w_P variation.

content of the soils was determined by the mass loss on ignition test follows the procedures outlined in BS 1377–3:2018 (BSI, 2018c). As the amount of the soil from the oedometer sample (about 150 g) was insufficient for the cone penetrometer test (300 g, as specified in British Standards Institution (BSI) (1990) and 200 g as specified in BSI (2018b)), additional soil samples were prepared and conditioned in the same way as the oedometer sample for the classification tests on the tested soils.

3. Test results

3.1. Compression/ swelling index variation

The compression (C_C) and swelling (C_S) indexes were calculated using test data from the one-dimensional consolidation test generally complied to BS EN ISO 17892-5:2017 (BSI, 2017). Fig. 4 shows the compression and swelling indexes of the test samples after various numbers of freezing and thawing cycles – the trends for the reconstituted Bothkennar and the destructured Bothkennar do not appear significantly different based on a visual inspection of the plot. However, the difference in C_C and C_S values between the reconstituted and destructured tests for a specific number of freeze-thaw cycles are comparable to the effects of different numbers of freezing and thawing cycles. Graham and Au (1985) showed a reduction in the compression index of natural plastic clay after one freeze-thaw cycle. In this experimental investigation, the measured C_C values from four sample series all exhibited a generally decreasing trend over an increasing number of freeze-thaw cycles, with most changes occurring during the first 7 cycles. The standard deviation values for the C_C of samples conditioned with various cycles of freezing and thawing are: 0.13 for reconstituted Kaolin, 0.092 for destructured Bothkennar, 0.036 for reconstituted Bothkennar, and 0.047 for reconstituted Gault clay. The reductions in C_C after 25 cycles for each sample series are 0.59 (unfrozen) to 0.21 (after 25 cycles) (reduced by 64%) for reconstituted Kaolin, 0.66 (unfrozen) to 0.43 (after 25 cycles) (reduced by 35%) for the destructured Bothkennar sample, 0.41 (unfrozen) to 0.29 (after 25 cycles) (reduced by 30%) for the

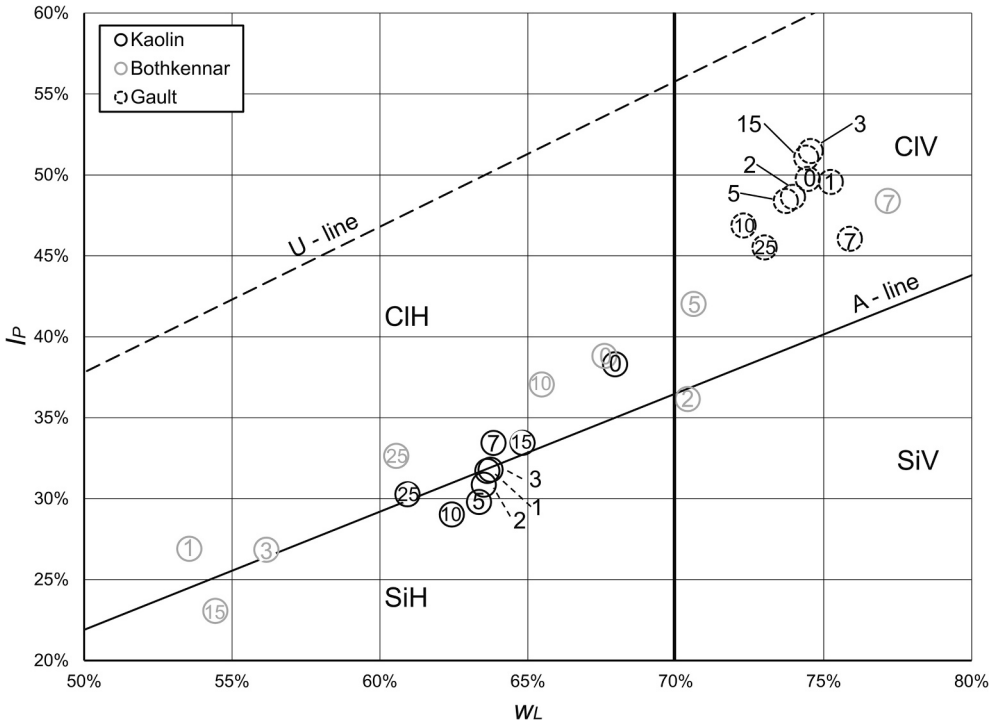

Fig. 6. Plasticity variation in a Casagrande chart (SiH: high plasticity silt, ClH: high plasticity clay, SiV: very high plasticity silt, ClV: very high plasticity clay) (number of freeze-thaw cycles are shown in the markers).

reconstituted Bothkennar sample, 0.43 (unfrozen) to 0.28 (after 25 cycles) (reduced by 35%) for the reconstituted Gault clay sample. The results show that the conditioning affects the C_C, which means that the changes in voids will not be as significant in soil after multiple (i.e., 25) cycles of freezing and thawing compared to the same soil at its unfrozen state. Some reductions in the swelling index (C_S) after 25 cycles can also be observed in all sample series, however the changes are relatively minor compared to the C_C. The standard deviation values of the C_S of samples conditioned with various cycles of freezing and thawing are: 0.016 for reconstituted Kaolin, 0.011 for destructured Bothkennar, 0.0045 for reconstituted Bothkennar, and 0.012 for reconstituted Gault clay. Prior studies showed that the C_C is related to parameters such as the initial w, the initial e, the w_L and w_p (e.g., Terzaghi and Peck (1948), Nishida (1956), Koppula (1981), Nagaraj and Srinivasa Murthy (1986), Al-Khafaji and Andersland (1992), Park and Koumoto (2004)). Therefore the variation of the measured soil index parameters due to freezing and thawing cycles are examined in the following sections.

3.2. Atterberg limits

Yong et al. (1985) examined the w_L of Matagami clay conditioned with freezing and thawing up to 32 cycles and reported a general decreasing trend of w_L over freeze-thaw cycles. Fig. 5 presents the variation of w_L, w_p of the tested soils subjected from 0 to 25 freeze-thaw cycles. The standard deviation values for the w_L of samples conditioned with various cycles of freezing and thawing are: 1.9% for Kaolin, 8.3% for Bothkennar clay, and 1.1% for Gault clay. The standard deviation values for the w_P are 1.3% for Kaolin, 2.2% for Bothkennar clay, and 2.1% for Gault clay. The w_L values of the tested soils exhibit an overall decreasing trend, but to varying degrees depending on the soil type. The decrease in w_L due to freeze-thaw cycles generally follows the trend observed for the C_C, whereas no systematic variation trend in w_p was observed for the tested soils over the increasing number of freeze thaw cycles (see Fig. 5). Fig. 6 presents the variation of Atterberg limits over different freeze thaw cycles in a Casagrande plasticity chart (all soils plot above "A-line" in the unfrozen state). Changes in plasticity over different freeze thaw cycles are limited for Kaolin and Gault clay, while the plasticity in Bothkennar clay after different cycles of freeze-thaw varies across four different soil classes (SiH: high plasticity silt, ClH: high plasticity clay, SiV: very high plasticity silt, ClV: very high plasticity clay) (these classification categories are defined in BSI (2018a)). Still, there appears to be no systematic variation between the plasticity index (I_P), soil characteristics, and freeze-thaw cycles based on the experimental data presented in this paper.

3.3. Transformation model linking k with w/w_L

The experimental results are examined using the transformation model established based on the study of the database FG/KSAT-1358 in Feng and Vardanega (2019b), to determine if the general trend of changes in k along with the other soil parameters continue to hold for soils conditioned with multiple cycles of freezing and thawing. Comparison of new test data with a large database allows the researcher to determine if the observed trends are comparable with those for a variety of soil types. Due to the potential discrepancies among the k values measured from different assessment methods (e.g., Moulton and Seals (1979), Tavenas et al. (1983)), the form of transformation model presented in this section is calibrated using the data subset for which the k was assessed from oedometer (one dimensional consolidation) tests ($n = 512$). The k data measured from soil samples conditioned with different numbers of cycles were regressed against w/w_L (using the natural logarithm of both correlates) to compare the new data to the results given in Feng and Vardanega (2019a, 2019b). The calibrated transformation models are summarised in Table 5. Both the w_L at unfrozen state (referred to in this paper as 'uncorrected' w_L) and the w_L measured after the identical number of freeze-thaw cycle as the k (referred to in this paper as 'corrected' w_L) were used in analysis. Fig. 7 shows the variation of the regression coefficients and exponents over 25 cycles of freeze thaw for four different sample types. The regression coefficients and exponents for Bothkennar clay and Gault clay show an increasing trend during the first 10 cycles, followed by a slight drop between 10 cycles to 25 cycles. The effect of sample state was not

Table 5
Summary of calibrated transformation models on sample conditioned over different freeze-thaw cycles.

Freeze-thaw cycle	Data source	Equation	R^2	n	Rearranged Equations
Unfrozen	unfrozen W_L	$\ln(k) = 3.62\ln(w/w_L) - 19.65$	0.64	39	$k = 2.92 \times 10^{-9}(w/w_L)^{3.62}$
1 cycle	unfrozen W_L	$\ln(k) = 5.11\ln(w/w_L) - 18.29$	0.62	20	$k = 1.14 \times 10^{-8}(w/w_L)^{5.11}$
	corrected W_L	$\ln(k) = 3.41\ln(w/w_L) - 19.79$	0.39	20	$k = 2.54 \times 10^{-9}(w/w_L)^{3.41}$
2 cycles	unfrozen W_L	$\ln(k) = 5.62\ln(w/w_L) - 17.61$	0.88	22	$k = 2.25 \times 10^{-8}(w/w_L)^{5.62}$
	corrected W_L	$\ln(k) = 5.24\ln(w/w_L) - 17.84$	0.85	22	$k = 1.79 \times 10^{-8}(w/w_L)^{5.24}$
3 cycles	unfrozen W_L	$\ln(k) = 4.42\ln(w/w_L) - 18.53$	0.75	24	$k = 8.96 \times 10^{-9}(w/w_L)^{4.42}$
	corrected W_L	$\ln(k) = 3.92\ln(w/w_L) - 19.34$	0.74	24	$k = 3.99 \times 10^{-9}(w/w_L)^{3.92}$
5 cycles	unfrozen W_L	$\ln(k) = 6.22\ln(w/w_L) - 16.63$	0.83	20	$k = 5.99 \times 10^{-8}(w/w_L)^{6.22}$
	corrected W_L	$\ln(k) = 6.28\ln(w/w_L) - 16.57$	0.86	20	$k = 6.36 \times 10^{-8}(w/w_L)^{6.28}$
7 cycles	unfrozen W_L	$\ln(k) = 5.49\ln(w/w_L) - 17.1$	0.80	26	$k = 3.75 \times 10^{-8}(w/w_L)^{5.49}$
	corrected W_L	$\ln(k) = 5.53\ln(w/w_L) - 16.69$	0.75	26	$k = 5.64 \times 10^{-8}(w/w_L)^{5.53}$
10 cycles	unfrozen W_L	$\ln(k) = 5.99\ln(w/w_L) - 16.91$	0.70	15	$k = 4.53 \times 10^{-8}(w/w_L)^{5.99}$
	corrected W_L	$\ln(k) = 5.97\ln(w/w_L) - 17.11$	0.70	15	$k = 3.71 \times 10^{-8}(w/w_L)^{5.97}$
15 cycles	unfrozen W_L	$\ln(k) = 6.56\ln(w/w_L) - 16.56$	0.78	15	$k = 6.43 \times 10^{-8}(w/w_L)^{6.56}$
	corrected W_L	$\ln(k) = 4.56\ln(w/w_L) - 18.68$	0.60	15	$k = 7.72 \times 10^{-9}(w/w_L)^{4.56}$
25 cycles	unfrozen W_L	$\ln(k) = 4.43\ln(w/w_L) - 18.41$	0.55	20	$k = 1.01 \times 10^{-8}(w/w_L)^{4.43}$
	corrected W_L	$\ln(k) = 3.85\ln(w/w_L) - 19.13$	0.48	20	$k = 4.92 \times 10^{-9}(w/w_L)^{3.85}$
Oedometer test data in FG/KSAT-1358 (Feng and Vardanega (2019))		$\ln(k) = 3.75\ln(w/w_L) - 20.72$	0.75	512	$k = 1.00 \times 10^{-9}(w/w_L)^{3.75}$

detected as when the reconstituted and destructured Bothkennar data are examined on Fig. 7, no signification deviation in the general trend is observed between these test series (the coefficient values tend to be slightly higher for the reconstituted tests with the exponent values being similar). It should be noted that the trends discussed in this section may be different for other datasets conducted with a wider range of freeze-thaw cycles and/or with varying sample state/condition.

4. Comparison of new laboratory data with the FG/KSAT-1358 database

Fig. 8 shows the ln(k) versus ln(w/w_L) plot for the experimental data with the 'corrected' w_L and the oedometer data from the database FG/KSAT-1358. The full database FG/KSAT-1358 is also presented for comparison. The experimental data from this test campaign overall follow the trend exhibited from both the full database FG/KSAT-1358, and the oedometer test data subset. Whilst the slope of the model generated from only the laboratory data are slightly lower than the oedometer data subset, the inclusion of laboratory data into the oedometer data subset and the full database FG/KSAT-1358 did not significantly influence the fitted model coefficient (oedometer test data subset $n = 512$, laboratory data from this study $n = 201$). The addition of almost 40% extra data points combined with the little changes of the fitting coefficient indicates that the previously observed trend is not been significantly influenced by the addition data of freeze-thaw conditioned samples. The updated transformation model (Eq. 4a) with the new laboratory k data combined oedometer data subset from FG/KSAT-1358 is:

$$lnk = 3.739ln(w/w_L) - 20.251 \left[R^2 = 0.63, n = 713, SE = 1.34, p < 0.0001\right] \quad (4a)$$

which can be re-arranged to:

$$k(m/s) = 1.60 \times 10^{-9}(w/w_L)^{3.739} \quad (4b)$$

The variation between Eq. (2) (coefficient: 1.00×10^{-9}, exponent: 3.75) and the updated transformation model (Eq. 4b, coefficient: 1.60×10^{-9}, exponent: 3.739) does not appear to be significant. The k-measured versus k-predicted plot (Fig. 9a) shows that the updated correlation (Eq. 4) with both the laboratory data and the oedometer data allows for estimation of k between 0.1 and 10 times of the measured value about 91% of the time (based on the data analysed in this paper) and give relatively evenly distributed predictions (54% overprediction versus 46% underprediction).

The updated transformation model (Eq. 5a) with the laboratory k data combined with the FG/KSAT-1358 data is:

$$ln(k) = 3.981ln(w/w_L) - 19.965 \left[R^2 = 0.59, n = 1553, SE = 1.57, p < 0.0001\right] \quad (5a)$$

which can be re-arranged to:

$$k(m/s) = 2.13 \times 10^{-9}(w/w_L)^{3.981} \quad (5b)$$

The variation between Eq. (1) (coefficient: 1.91×10^{-9}, exponent: 4.083) and the updated transformation model (Eq. 5b, coefficient: 2.13×10^{-9}, exponent: 3.981) are relatively minor. Fig. 9b presents the k-measured versus k-predicted plot based on Eq. (5). The result shows that the updated equation with the inclusion of laboratory data allows 89% of the predictions to fall within the 0.1 to 10 times range and tends to give slightly overpredicted results with 57% of measurements overpredicted and 43% underpredicted.

5. Summary and conclusions

This paper has presented new laboratory data from tests on four fine-grained sample series, reconstituted Kaolin, destructured Bothkennar clay, reconstituted Bothkennar clay, and reconstituted Gault clay. The soil samples were submerged in de-ionized water for 24 h before being subjected to freezing and thawing conditioning. The soil samples were conditioned in an oedometer cell while being subjected to varying numbers of freezing and thawing up to 25 cycles. The influence of freeze-thaw cycles on key soil parameters, including the compression and swelling indices (C_C, C_S), the Atterberg limits (w_L, w_P), were examined. The k test results of the sample series over different numbers of freezing and thawing were analysed following the form of the k transformation model (Eq. 1) developed from FG/KSAT-1358 presented in Feng and Vardanega (2019b). The results were then compared with the analysis of the previously published database on k on fine-grained soils (FG/KSAT-1358). While the multiple cycles of freezing and thawing appear to affect some soil parameters, such as the Atterberg limits and the compression characteristics, the effects on the transformation model parameters, linking w/w_L to k are less apparent.

The main findings from this research work are:

- For the soils studied in this paper, a gradual reduction of w_L may be expected over multiple cycles of freezing and thawing with similar trends observed for the C_C. The reconstituted Bothkennar and the destructured Bothkennar show a similar general trend of C_C decreasing over multiple cycles of freezing and thawing but this decrease is of a similar magnitude to the difference in C_C values between the two sample states.

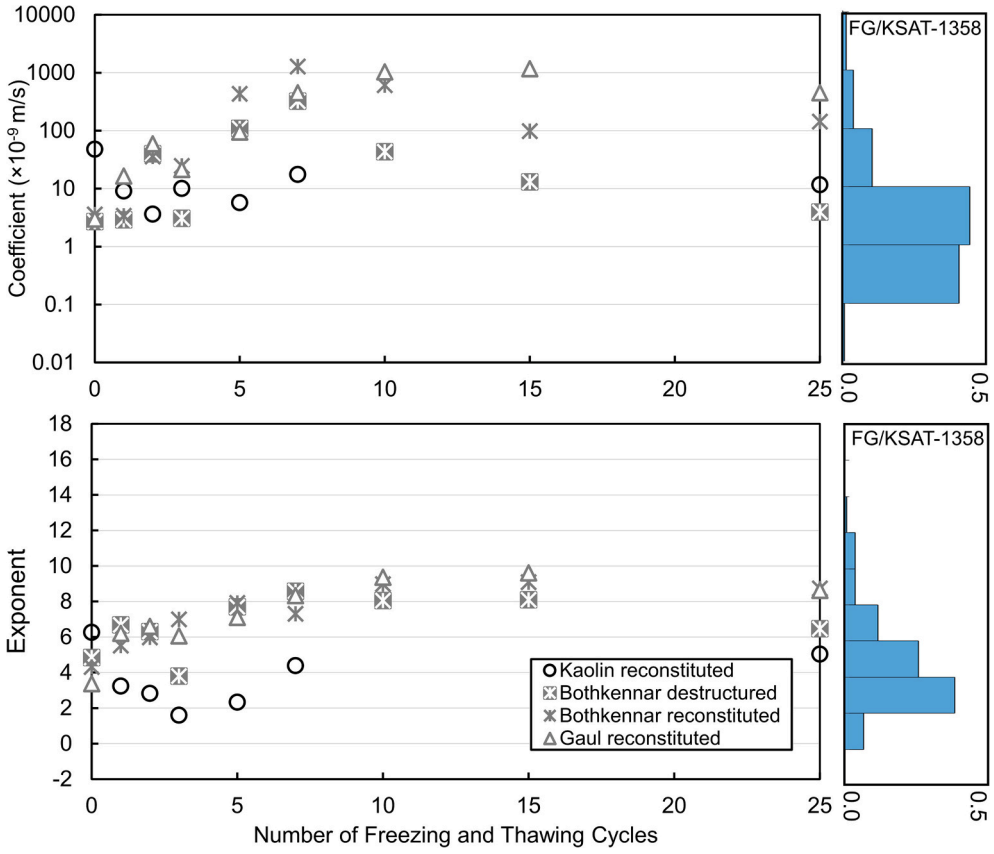

Fig. 7. Variation of the regression coefficients and exponents over increasing number of freezing/thawing cycles.

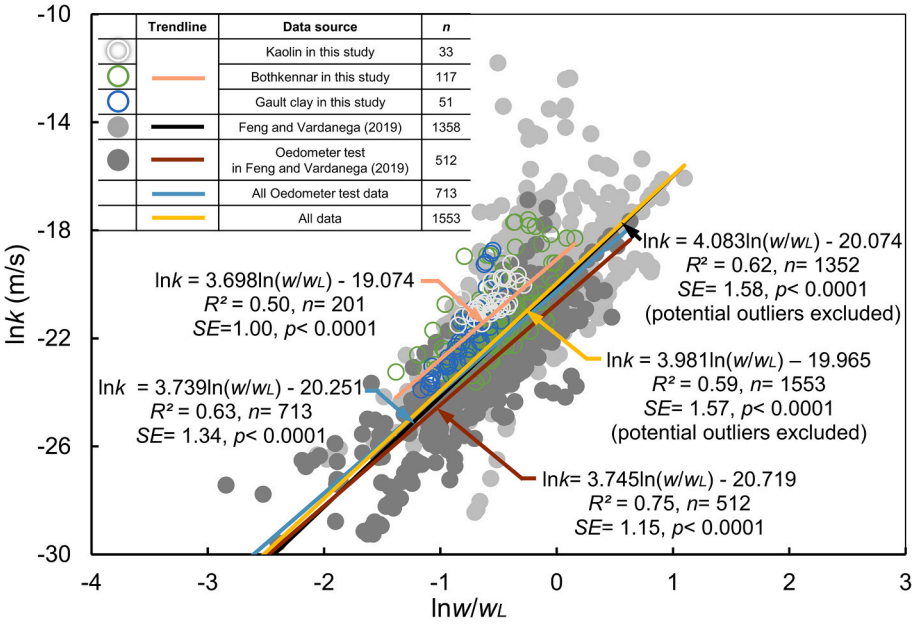

Fig. 8. ln(k) plotted against ln(w/w_L) in comparison with FG/KSAT-1358 (fitted correlation for each tested sample type can be found in Fig. S17 of the supplemental data).

- The transformation model coefficients and exponents for Bothkennar and Gault show an increase during the first 10 cycles, followed by a slight drop between 10 and 25 cycles. The effect of sample state was not detected although the coefficient values tended to be slightly higher for the reconstituted Bothkennar tests as compared to the destructured ones.
- When the data from FG/KSAT-1358 is combined with the new experimental data from this study there only minor changes in the transformation model coefficients were observed (e.g. comparison of Eq. 1 and 5b shows that the exponent changes from 4.083 to 3.981 and that the coefficient changes from 1.91×10^{-9} to 2.13×10^{-9}). The R^2 for the regression used to develop Eq. 1 in Feng and

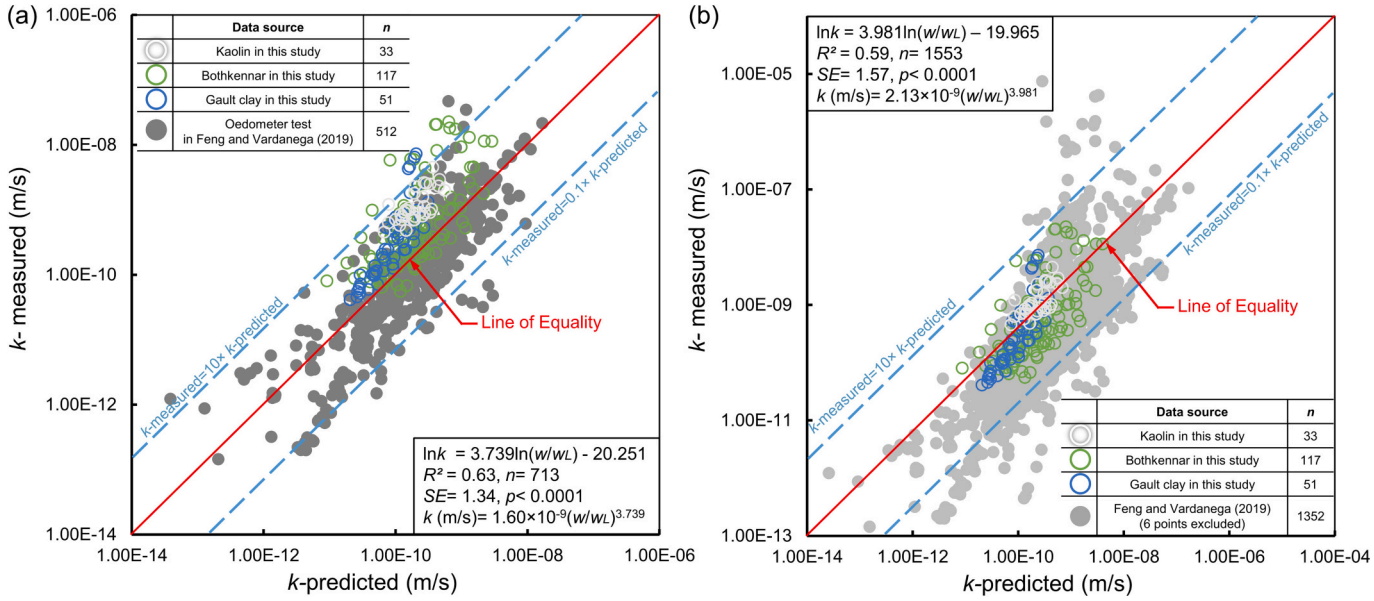

Fig. 9. *k*-measured plotted against *k*-predicted: (a) with the oedometer test data subset, (b) with the entire database FG/KSAT-1358.

Vardanega (2019b) was 0.62, this value decreases slightly to 0.59 for Eq. 5a. The inclusion of over 200 new data-points does not significantly affect Eq. 1 (or indeed Eq. 2) and the robustness of the transformation model is not significantly impacted by the addition of this new data.

This last finding is of practical use for geotechnical and pavement engineers working in cold regions as the transformation models established by the large FG/KSAT-1358 database can still be used for prediction of *k*. The study shows the ability of the transformation models developed in Feng and Vardanega (2019a, 2019b) which can reduce the uncertainty of the *k* of fine-grained soils by about five orders of magnitude (i.e., from around seven to two) to also be effective in reducing the uncertainty of *k* for soils subjected to multiple cycles of freezing and thawing. This literature review from this study demonstrated that there is a lack of hydraulic conductivity data for soil samples conditioned with a high number of freeze-thaw cycles (i.e., over 25 cycles), and therefore, further work is needed in this area.

Declaration of Competing Interest

The authors declare that they have no known competing financial interests or personal relationships that could have appeared to influence the work reported in this paper.

Data availability

Underlying laboratory testing data has been supplied along with the supplemental materials for this paper.

Acknowledgements

The first author thanks Dr. S. Kearns from the University of Bristol for helpful discussions related to the SEM images, and Mr. G. Martin from the University of Bristol for technical support during the geotechnical laboratory testing programme. The first author acknowledges the support from the China Scholarship Council (201708060067) during her doctoral studies at the University of Bristol.

Appendix A. Supplementary data

Supplementary data to this article can be found online at https://doi.org/10.1016/j.coldregions.2023.103902.

References

Al-Khafaji, A.W.N., Andersland, O.B., 1992. Equations for compression index approximation. J. Geotech. Eng. ASCE 118 (1), 148–153. https://doi.org/10.1061/(ASCE)0733-9410(1992)118:1(148).

Benson, C.H., Othman, M.A., 1993. Hydraulic conductivity of compacted clay frozen and thawed in situ. J. Geotech. Eng. ASCE 119 (2), 276–294. https://doi.org/10.1061/(ASCE)0733-9410(1993)119:2(276).

Benson, C.H., Abichou, T.H., Olson, M.A., Bosscher, P.J., 1995. Winter effects on hydraulic conductivity of compacted clay. J. Geotech. Eng. ASCE 121 (1), 69–79. https://doi.org/10.1061/(ASCE)0733-9410(1995)121:1(69).

Bowders, J., McClelland, S., 1994. The effects of freeze/thaw cycles on the permeability of three compacted soils. In: Hydraulic Conductivity and Waste Contaminant Transport in Soil. ASTM International, West Conshohocken, PA, pp. 461–481. https://doi.org/10.1520/STP23903S.

British Standards Institution (BSI), 1990. Methods of test for soils for civil engineering purposes - Part2: Classification tests. In: BS 1377–2:1990. BSI, London, UK.

BSI, 1990. Methods of test for soils for civil engineering purposes - Part 5: Compressibility, permeability and durability tests. In: BS 1377–5:1990. BSI, London, UK.

BSI, 2017. Geotechnical investigation and testing - Laboratory testing of soil. Part 5: Incremental loading oedometer test. BSI, London, UK.

BSI, 2018a. Geotechnical investigation and testing - Identification and classification of soil. Part 2: Principles for a classification. BSI, London, UK.

BSI, 2018b. Geotechnical investigation and testing - Laboratory testing of soil Part 12: Determination of liquid and plastic limits. BSI, London, UK.

BSI, 2018c. Methods of test for soils for civil engineering purposes - Chemical and electro-chemical testing. In: BS 1377–3:2018. BSI, London, UK.

Carrier, W.D., Beckman, J.F., 1984. Correlations between index tests and the properties of remoulded clays. Géotechnique 34 (2), 211–228. https://doi.org/10.1680/geot.1984.34.2.211.

Chamberlain, E.J., Gow, A.J., 1979. Effect of freezing and thawing on the permeability and structure of soils. Eng. Geol. 13 (1–4), 73–92. https://doi.org/10.1016/0013-7952(79)90022-X.

Chamberlain, E.J., Iskandar, I., Hunsicker, S.E., 1990. Effect of freeze-thaw cycles on the permeability and macrostructure of soils. In: Cooley, K.R. (Ed.), Proceedings of International Symposium on Frozen Soil Impacts on Agricultural, Range, and Forest Lands. Cold Region Research and Engineering Laboratory, Spokane, WA, pp. 145–155. https://apps.dtic.mil/sti/pdfs/ADA219687.pdf#page=151 [15/05/2023].

Chapuis, R.P., 2012. Predicting the saturated hydraulic conductivity of soils: A review. Bull. Eng. Geol. Environ. 71 (3), 401–434. https://doi.org/10.1007/s10064-012-0418-7.

Craig, R.F., 2004. Craig's Soil Mechanics. Taylor & Francis, Abingdon, UK.

Dawson, A., 2009. Water in Road Structures, 5. Springer, Netherlands. https://doi.org/10.1007/978-1-4020-8562-8.

Eigenbrod, K.D., Knutsson, S., Sheng, D., 1996. Pore-Water Pressures in Freezing and Thawing Fine-Grained Soils. J. Cold Regions Eng. 10 (2), 77–92. https://doi.org/10.1061/(ASCE)0887-381X(1996)10:2(77).

Feng, S., 2022. Hydraulic Conductivity of Road Construction Materials: with a Focus on Freeze-thaw Effects. Ph.D. thesis. University of Bristol, Bristol, UK.

Feng, S., Vardanega, P.J., 2019a. A database of saturated hydraulic conductivity of fine-grained soils: probability density functions. Georisk 13 (4), 255–261. https://doi.org/10.1080/17499518.2019.1652919.

Feng, S., Vardanega, P.J., 2019b. Correlation of the hydraulic conductivity of fine-grained soils with water content ratio using a database. Environ. Geotech. 6 (5), 253–268. https://doi.org/10.1680/jenge.18.00166.

Feng, S., Ibraim, E., Vardanega, P.J., 2022. Databases to assess the hydraulic conductivity of road construction materials. In: Rahman, M.M., Jaksa, M. (Eds.), Proceedings of the 20th International Conference on Soil Mechanics and Geotechnical Engineering –, Australian Geomechanics Society, Sydney, Australia, May 1–5, 2022, vol. 2, pp. 4547–4552.

Forster, A., Hobbs, P.R.N., Cripps, A.C., Entwistle, D.C., Fenwick, S.M.M., Raines, M.R., Hallam, J.R., Hones, L.D., Self, S.J., Meakin, J.L., 1995. Engineering geology of British rocks and soils: Gault Clay. In: British Geological Survey, Nottingham, UK. https://www.bgs.ac.uk/download/engineering-geology-of-british-rocks-and-soils-gault-clay/# [25/05/2023].

Graham, J., Au, V.C.S., 1985. Effects of freeze–thaw and softening on a natural clay at low stresses. Can. Geotech. J. 22 (1), 69–78. https://doi.org/10.1139/t85-007.

Henry, H.A.L., 2007. Soil freeze–thaw cycle experiments: Trends, methodological weaknesses and suggested improvements. Soil Biol. Biochem. 39 (5), 977–986. https://doi.org/10.1016/j.soilbio.2006.11.017.

Hewitt, R.D., Daniel, D.E., 1997. Hydraulic conductivity of geosynthetic clay liners after freeze-thaw. J. Geotech. Geoenviron. Eng. ASCE 123 (4), 305–313. https://doi.org/10.1061/(asce)1090-0241(1997)123:4(305).

Hight, D.W., Bond, A.J., Legge, J.D., 1992. Characterization of the Bothkennar clay: An overview. Géotechnique 42 (2), 303–347. https://doi.org/10.1680/geot.1992.42.2.303.

Hohmann-Porebska, M., 2002. Microfabric effects in frozen clays in relation to geotechnical parameters. Appl. Clay Sci. 21 (1–2), 77–87. https://doi.org/10.1016/S0169-1317(01)00094-1.

Jamshidi, R.J., Lake, C.B., 2015. Hydraulic and strength properties of unexposed and freeze–thaw exposed cement-stabilized soils. Can. Geotech. J. 52 (3), 283–294. https://doi.org/10.1139/cgj−2014-0100.

Jamshidi, R.J., Lake, C.B., Barnes, C.L., 2015. Examining freeze/thaw cycling and its impact on the hydraulic performance of cement-treated silty sand. J. Cold Regions Eng. 29 (3), [04014014]. https://doi.org/10.1061/(asce)cr.1943-5495.0000081.

Jones, C.W., 1987. Long-term Changes in the Properties of Soil Linings for CANAL SEEPAGE CONTROL. Report no. REC-ERC-87-1. Bureau of Reclamation, Engineering and Research Center, Denver, CO.

Kim, W., Daniel, D.E., 1992. Effects of freezing on hydraulic conductivity of compacted clay. J. Geotech. Eng. ASCE 118 (7), 1083–1097. https://doi.org/10.1061/(ASCE)0733-9410(1992)118:7(1083).

Konrad, J.-M., 1989. Physical processes during freeze-thaw cycles in clayey silts. Cold Reg. Sci. Technol. 16 (3), 291–303. https://doi.org/10.1016/0165-232X(89)90029-3.

Konrad, J.-M., 2010. Hydraulic conductivity changes of a low-plasticity till subjected to freeze–thaw cycles. Géotechnique 60 (9), 679–690. https://doi.org/10.1680/geot.08.P.020.

Konrad, J.-M., Samson, M., 2000. Hydraulic conductivity of kaolinite-silt mixtures subjected to closed-system freezing and thaw consolidation. Can. Geotech. J. 37 (4), 857–869. https://doi.org/10.1139/t00-003.

Koppula, S., 1981. Statistical estimation of compression index. Geotech. Test. J. 4 (2), 68–72. https://doi.org/10.1520/GTJ10768J.

Kuriakose, B., Abraham, B.M., Sridharan, A., Jose, B.T., 2017. Water content ratio: an effective substitute for liquidity index for prediction of shear strength of clays. Geotech. Geol. Eng. 35 (4), 1577–1586. https://doi.org/10.1007/s10706-017-0193-0.

LaPlante, C.M., Zimmie, T.F., 1992. Freeze/Thaw Effects on the Hydraulic Conductivity of Compacted Clays. Transportation Research Record 1369, pp. 126–129. Available from: https://onlinepubs.trb.org/Onlinepubs/trr/1992/1369/1369-016.pdf [25/05/2023].

Leroueil, S., Tavenas, F., Locat, J., 1985. Discussion: Correlations between index tests and the properties of remoulded clays. Géotechnique 35 (2), 223–226. https://doi.org/10.1680/geot.1985.35.2.223.

Makusa, G., Mácsik, J., Holm, G., Knutsson, S., 2016. Laboratory test study on the effect of freeze–thaw cycles on strength and hydraulic conductivity of high water content stabilized dredged sediments. Can. Geotech. J. 53 (6), 1038–1045. https://doi.org/10.1139/cgj-2015-0295.

Mallick, R.B., El-Korchi, T., 2008. Pavement Engineering: Principles and Practice. CRC Press, Boca Raton, FL.

Mbonimpa, M., Aubertin, M., Chapuis, R., Busssière, B., 2002. Practical pedotransfer functions for estimating the saturated hydraulic conductivity. Geotech. Geol. Eng. 20 (3), 235–259. https://doi.org/10.1023/A:1016046214724.

McDowall, I.C., 1960. Particle size reduction of clay minerals by freezing and thawing. N. Z. J. Geol. Geophys. 3 (3), 337–343. https://doi.org/10.1080/00288306.1960.10422079.

Moulton, L., Seals, D., 1979. Determination of the In Situ Permeability of Base and Subbase Courses. Report no. FHWA-RD-79-88. Federal Highway Administration, U. S. Department of Transportation, Washington, D.C., USA. Available from: https://rosap.ntl.bts.gov/view/dot/30030 [25/05/2023].

Nagaraj, T.S., Srinivasa Murthy, B.R., 1986. A critical reappraisal of compression index equations. Géotechnique 36 (1), 27–32. https://doi.org/10.1680/geot.1986.36.1.27.

Nagaraj, T.S., Pandian, N.S., Narasimha Raju, P.S.R., 1993. Stress state-permeability relationships for fine-grained soils. Géotechnique 43 (2), 333–336. https://doi.org/10.1680/geot.1993.43.2.333.

Nagaraj, T.S., Pandian, N.S., Raju, P.S.R.N., 1994. Stress state-permeability relations for overconsolidated clays. Géotechnique 44 (2), 349–352. https://doi.org/10.1680/geot.1994.44.2.349.

Nash, D.F.T., Powell, J.J.M., Lloyd, I.M., 1992. Initial investigations of the soft clay test site at Bothkennar. Géotechnique 42 (2), 163–181. https://doi.org/10.1680/geot.1992.42.2.163.

Nishida, Y., 1956. A Brief Note on Compression Index of Soil. J. Soil Mech. Found. Division 82 (3), 295–316. https://doi.org/10.1061/JSFEAQ.0000015.

Olek, B.S., 2019. Critical reappraisal of Casagrande and Taylor methods for coefficient of consolidation. KSCE J. Civ. Eng. 23 (9), 3818–3830. https://doi.org/10.1007/s12205-019-1222-8.

Othman, M.A., Benson, C.H., 1993. Effect of freeze-thaw on the hydraulic conductivity and morphology of compacted clay. Can. Geotech. J. 30 (2), 236–246. https://doi.org/10.1139/t93-020.

Park, J.H., Koumoto, T., 2004. New compression index equation. J. Geotech. Geoenviron. Eng. ASCE 130 (2), 223–226. https://doi.org/10.1061/(ASCE)1090-0241(2004)130:2(223).

Paul, M.A., Peacock, J.D., Wood, B.F., 1992. The engineering geology of the carse clay at the national soft clay research site. Bothkennar. *Géotechnique* 42 (2), 183–198. https://doi.org/10.1680/geot.1992.42.2.183.

Pennington, D.S., 1999. The anisotropic small strain stiffness of Cambridge Gault clay. Ph.D. thesis. University of Bristol, Bristol, UK.

Prasad, M.S., Reid, K.J., Murray, H.H., 1991. Kaolin: processing, properties and applications. Appl. Clay Sci. 6 (2), 87–119. https://doi.org/10.1016/0169-1317(91)90001-P.

Sarsembayeva, A., Collins, P.E.F., 2017. Evaluation of frost heave and moisture/chemical migration mechanisms in highway subsoil using a laboratory simulation method. Cold Reg. Sci. Technol. 133, 26–35. https://doi.org/10.1016/j.coldregions.2016.10.003.

Simonsen, E., Isacsson, U., 1999. Thaw weakening of pavement structures in cold regions. Cold Reg. Sci. Technol. 29 (2), 135–151. https://doi.org/10.1016/S0165-232X(99)00020-8.

Sivapullaiah, P.V., Sridharan, A., Stalin, V.K., 2000. Hydraulic conductivity of bentonite–sand mixtures. Can. Geotech. J. 37 (2), 406–413. https://doi.org/10.1139/t99-120.

Sterpi, D., 2015. Effect of freeze–thaw cycles on the hydraulic conductivity of a compacted clayey silt and influence of the compaction energy. Soils Found. 55 (5), 1326–1332. https://doi.org/10.1016/j.sandf.2015.09.030.

Sukolrat, J., 2007. Structure and Destructuration of Bothkennar Clay. Ph.D. thesis. Univerisity of Bristol, Bristol, UK.

Tang, Y.Q., Yan, J.J., 2015. Effect of freeze–thaw on hydraulic conductivity and microstructure of soft soil in Shanghai area. Environ. Earth Sci. 73 (11), 7679–7690. https://doi.org/10.1007/s12665-014-3934-x.

Tavenas, F., Leblond, P., Jean, P., Leroueil, S., 1983. The permeability of natural soft clays. Part I: Methods of laboratory measurement. Can. Geotech. J. 20 (4), 629–644. https://doi.org/10.1139/t83-072.

Taylor, D.W., 1948. Fundamentals of Soil Mechanics. John Wiley & Sons Inc., New York, NY.

Terzaghi, K., Peck, R.B., 1948. Soil Mechanics in Engineering Practice. John Wiley & Sons, New York, NY.

Thom, N., 2014. Principles of Pavement Engineering, (Second Edition). ICE Publishing, London, UK. https://doi.org/10.1680/ppe.58538.

Tripathy, S., Al-Hussaini, O.M., Cleall, P.J., Rees, S.W., Wang, H.L., 2020. Frost heave and thaw settlement of initially saturated-slurried and compacted-saturated materials. E3S Web Conf. 195, [03036]. https://doi.org/10.1051/e3sconf/202019503036.

Viklander, P., 1997. Compaction and Thaw Deformation of Frozen Soil: Permeability and Structural Effects due to Freezing and Thawing. Ph.D. thesis.. Luleå University of Technology, Luleå, Sweden.

Viklander, P., 1998. Permeability and volume changes in till due to cyclic freeze/thaw. Can. Geotech. J. 35 (3), 471–477. https://doi.org/10.1139/t98-015.

Viklander, P., Eigenbrod, D., 2000. Stone movements and permeability changes in till caused by freezing and thawing. Cold Reg. Sci. Technol. 31 (2), 151–162. https://doi.org/10.1016/S0165-232X(00)00009-4.

Wong, L.C., Haug, M.D., 1991. Cyclical closed-system freeze–thaw permeability testing of soil liner and cover materials. Can. Geotech. J. 28 (6), 784–793. https://doi.org/10.1139/t91-095.

Yong, R.N., Boonsinsuk, P., Yin, C.W.P., 1985. Alteration of soil behaviour after cyclic freezing and thawing. In: Seiichi, K., Masam, F. (Eds.), Ground freezing: Proceedings of the Fourth International Symposium on Ground Freezing. A.A. Balkema, Japan, pp. 187–195.